Wet and dry spells in Senegal: Evaluation of satellite-based and model re-analysis rainfall estimates

Cheikh Modou Noreyni Fall[1], Christophe Lavaysse[2], Mamadou Simina Drame[1], Geremy Panthou[2], and Amadou Thierno Gaye[1]

[1]Laboratoire de Physique de l'Atmosphère et de l'Océan—Simeon Fongang, ESP, Univ. Cheikh Anta Diop, Dakar, Senegal
[2]Institut des Géosciences de l'Environnement IGE, Univ. Grenoble Alpes, IRD, CNRS, Grenoble INP, 38000 Grenoble, France

Correspondence: Noreyni Fall (noreyni27@gmail.com)

Abstract. In this study, wet and dry spells over Senegal provided by four datasets based on satellite data (TRMM-3B42 V7, TAMSAT V3, CMORPH V1.0, CHIRPS V2.0), two fully based on (re)analyses (NCEP-CFSR, ERA5) and one was fully based on gauge observations (CPC Unified V1.0/RT) are compared with respect to observation datasets derived from 65 rain gauge network. All datasets were converted to the same temporal and spatial scales with $0.25° \times 0.25°$ as resolution. Ordinary

5   kriging (OK) and block kriging (BK) were used for the spatial interpolation of the gauge data. Despite a spatial coherence of the seasonal rainfall accumulation between all products, more variability with intra-seasonal features are shown in this paper. The seasonal cycle of dry days shows that TRMM, CPC, ERA5, NCEP and OK record more dry days (from 45% to 55% of dry days in August) while TAMSAT, CHIRPS, CMORPH and BK record less dry day (from 40% to 30% of dry days in August). All datasets highlighted an agreement that dry spell indicator underscore often false start and early cessation of the

10   rainy Season in Senegal. Although, it can rarely occurs during intensification of West African monsoon (August-September). The most contrast is found on the detection of wet indicators intensity. Wet spell (defined as period with precipitation higher than a certain percentile of historical precipitation) are more severe in OK and TRMM than in other datasets. However, a great similarity is shown on their temporal frequencies.

15   An increase of extreme events is one of the main phenomena accompanying the rainfall recovery in Sahel (Alhassane et al., 2013; Descroix et al., 2016; Panthou et al., 2014, 2018; Wilcox et al., 2018). Several studies related to the effect of climate change, predict an intensification of hydrological cycle, and thus an increased probability of heavy rainfall and dry spell, associated with global warming (Held and Soden, 2008; Giorgi et al., 2011; Trenberth, 2011; Kendon et al., 2019; Berthou et al., 2019). Recently, extremes events have been occurred in West Africa such as an extreme rain event that occurred in

20   Burkina Faso on 1 September 2009 with an absolute record of 263 mm rainfall observed at Ouagadougou (Lafore et al., 2017). In Senegal, more than 26 people died due to the direct and indirect impacts of an extreme rainfall event on 26 August 2012 marked by 161 mm in less than 3 hours (Sagna et al., 2015).

Likewise, drought may cause important impacts as well. In 2014, a severe drought impacted several localities in Senegal which led Senegalese government to receive \$16.5 million funding from the African Risk Capacity (ARC, 2014). Indeed, the 2014/2015 agricultural season was marked by false start and long dry spells of the rainy season and also by poor, irregular and badly distributed rainfall throughout most of the country's territory. According to WFP (World Food Program) Country

5   Brief, Senegal is one of the seven Sahelian countries where the number of food-insecure people will increase significantly, from 314,600 people currently to 548,000 people during the 2018 lean season (WFP, 2018).

In this context of high risk associated with extreme hydro-meteorological events due to the high vulnerability of the population, it is important to better understand regime and multi-scale rainfall variability (Le Barbé et al., 2002; Lebel and Ali, 2009; Nicholson, 2013; Dione et al., 2014; Yeni and Alpas, 2017). Some studies using raingauges, rainfall estimates from

10   satellite imagery and Numerical Weather Prediction (NWP) have focused on the multi-scales variability of these potentially high-impact events (Washington et al., 2006; Sane et al., 2018; Nicholson et al., 2018). Indeed, in Sahel, since recovery, we observe the mixed dry/wet seasonal rainfall features which are called hybrid rainy seasons (Salack et al., 2016). These hybrid rainy seasons illustrating a rainfall intensification is part of what Giorgi et al. (2011) have defined as a more extreme hydrological climate, that is longer dry spells and more intense rainfall when it rains (Trenberth et al., 2003; Trenberth, 2011). Froidurot

15   and Diedhiou (2017) found that the spatio-temporal variability of the dry and wet periods also seems to be closely related to the spatial-temporal variability of the West African monsoon. In addition, the seasonal cycle of these longer dry periods has higher occurrences at the beginning and end of the rainy season, making them crucial in agro-climatic monitoring. Using a hierarchical cluster analysis throughout the 1951-1996 period in Senegal, Dieng et al. (2008) specified that at intra-seasonal time-scales, in the northern part of the country we observe that an earlier (later) long dry spell is associated with upper (lower) seasonal

20   rainfall amounts in July-August-September. However, there is no such relationship in the South. Hence, understanding these high-impact events and forecasting them may thus offer interesting applications in agronomy and also floods management.

Unfortunately, very few studies inter-compare the performance of satellite imagery, Numerical Weather Prediction (NWP) model outputs and ground observations on the distribution of wet and dry spell within the rainy season in Sahel (Knapp et al., 2011). Some studies have been conducted in Africa to focus essentially on rainfall inter-annual variability (Thorne et al., 2001;

25   Ali et al., 2005). Indeed, TAMSAT (Tropical Applications of Meteorology using satellite data and ground based observations V3) are better over plateau regions, with 59% estimates within 1 Standard error (s.e) of the rainfall, but over the whole region the CPC Unified V1.0/RT estimates perform best (Maidment et al., 2013). While, Dinku et al. (2007); Jobard et al. (2010) found that the NOAA-RFE 2.0 algorithm performs well in west Africa but poorly in Ethiopia. Conversely, the CMORPH algorithm shows good agreement with gauge data in Ethiopia but strongly underestimates rainfall amount in the Sahel.

30   The goal of this paper is to evaluate the performance of four datasets based on satellite data (TRMM-3B42 V7, TAMSAT V3, CMORPH V1.0, CHIRPS V2.0), two fully based on (re)analyses (NCEP-CFSR, ERA5), one was fully based on gauge observations (CPC Unified V1.0/RT) and two spatial interpolated of 65 rain gauges of ANACIM the National Agency of Civil Aviation and Meteorology (Table 1) on the detection and evolution of these extreme hazards. It focuses over Senegal, Sahelian country located from $11.21°W$ to $17.32°W$ and from $12.8°N$ to $16.41°N$ as illustrated in Fig. 1. Firstly, the spatial distribution

35   of seasonal rainfall accumulation and the seasonal cycle of dry days per month is analyzed. Secondly, dry indicators (DS and

DSC) and wet indicators are defined characterized (WS and WSC, Table 2 and Table 3). The paper is structured as follows. Section 2 provides a description of the data and the methodology used in our analysis, while section 3 presents the main results, along with statistical tests performed to determine if the observed features could have been by chance. Section 4 concludes the paper with a summary of our main findings.

1 Data and Methodological approach

1.1 Rain gauges data and kriging

Daily rain gauge data are provided by the national meteorological service of Senegal (ANACIM). To avoid in-homogeneity in time 65 stations are used to cover from 1991 to 2010 (see Fig. 1). Two levels of quality control have been done. A manual checks for suspicious records were carried out, then, further checks were performed including verification of station locations, identification of repeated data, identification of outliers, comparative tests using neighboring stations and investigation of suspicious zero values (i.e. missing data or zero rainfall). The rain gauge data were converted to the same spatial support using ordinary and block kriging (OK and BK). Several studies showed that Kriging is the most efficient interpolation methods (Creutin and Obled, 1982; Tabios and Salas, 1985; Goovaerts, 2000). In this case the double kriging approach was applied. Indicator kriging is used to define a rainy area and ordinary kriging illustrated by a equation 1 is used to calculate rainfall amount within the rainy area:

$$Z^k = \sum_{i=1}^{n} \lambda_i Z_i^o \tag{1}$$

where Z^k and Z^o represent respectively rainfall estimate and rain gauge value; λ_i are the weights assigned to the available n observations. One effect of the kriging rainfall is the reduction of high values and the increase of low values. To correct this bias, a Quantile-Mapping illustrated by the equation 2 is used.

$$F_o(x_o) = F_k(x_k) \Rightarrow x_q = F_o^{-1}[F_k(x_k)] \tag{2}$$

Where F_o is the distribution function observed; F_k the distribution function estimated; x_o the observed quantile; x_k the estimated quantile. The square root of the OK variance is used. The OK standard error serves as a measure of confidence in estimates across the region of interest (Grimes et al., 1999).

The another method of kriging used in this study is the block kriging (BK). it is a method aiming at estimate the spatial average of a process over given area. In this paper we use it to predict the areal rainfall (mean spatial) at the grid scale $0.25° \times 0.25°$ in order to compare with other datasets (Lloyd and Atkinson, 2001; Maidment et al., 2013).

1.2 Satellite and reanalysis and combined datasets

Since the purpose of this study is to compare occurrence and temporal distribution of wet and dry spells between available datasets and ground observations, an ensemble of 7 different datasets available are used.

TRMM-3B42 V7 (Tropical Rainfall Measuring Mission 3B42v7) are derived from a combination of microwave and infrared

5 radar estimated calibration (Kummerow et al., 1998; Nesbitt et al., 2006; Huffman et al., 2007). The TRMM 3B42 v7 data has a temporal resolution of 3 hours and $0.25° \times 0.25°$ as spatial resolution and covers a spatial area which extends from $50°S - 50°N$ and $0°W - 360°W$ covering the period from 1998 to 2013. Since its launch in 1997, TRMM provided rainfall measurement in tropical and subtropical regions.

TAMSAT-V3 (Tropical Applications of Meteorology using satellite data and ground based observations V3) is developed by

10 the University of Reading is based on the channel TIR (Thermal Infrared) Meteosat. The methodology for estimating TAMSAT is based on a linear relationship between the number of hours for which the temperature of a pixel is colder than a specified threshold called The Cold Cloud Duration (CSD) and the amount of rain (Grimes et al., 1999; Janowiak et al., 2001; Tarnavsky et al., 2014). The TAMSAT algorithm is calibrated locally using rainfall station data (Maidment et al., 2017).

CPC Unified Gauge-based Analysis of Global Daily Precipitation V1.0/RT use gauge reports from over 30,000 stations are

15 collected from multiple sources including GTS, COOP, and other national and international agencies. Quality controlled station reports are then interpolated to create analyzed fields of daily precipitation with consideration of orographic effects (Xie et al., 2017). The daily analysis is constructed on a 0.125 degree lat/lon grid over the entire global land areas for a period from 1979 to 2016.

CMORPH V1.0 (CPC Morphing Technique) produces global precipitation estimations at very high spatial and temporal resolu-

20 tion a spatial resolution of $0.25° \times 0.25°$ with a time resolution of 3 hours. These estimates are generated by algorithms SSM/I (Special sensor microwave/imagery), AMSU-B (Advanced microwave sounding unit) and TMI (Kummerow et al., 1998; Ferraro and Li, 2002; Ferraro, 1997). This method is extremely flexible such that any precipitation estimates from any microwave satellite source can be incorporated (Joyce et al., 2004; Zeweldi and Gebremichael, 2009; Xie et al., 2017).

CHIRPS V2.0 (Climate Hazards Group InfraRed Station with Precipitation data) is a 30+ year quasi-global rainfall dataset.

25 Spanning $50°S - 50°N$ (and all longitudes), starting in 1981 to near-present, CHIRPS incorporates $0.05°$ resolution satellite imagery with in-situ station data to create gridded daily rainfall time series for trend analysis and seasonal drought monitoring (Funk et al., 2015).

NCEP-CFSR daily data rainfall covering January 1979 through the present, are available on the T62 Gaussian grid with a spatial resolution of about $1.875° \times 1.875°$. NCEP Reanalysis precipitation is completely determined by the model and is a

30 variable produced with no direct impact from observations (Ebert et al., 2007; Saha et al., 2010).

ERA5 was produced using 4D-Var data assimilation in CY41R2 of ECMWF's Integrated Forecast System (IFS), with 137 hybrid sigma/pressure (model) levels in the vertical, with the top level at 0.01 hPa. "Surface or single level" data are also available, containing 2D parameters such as precipitation, 2m temperature, top of atmosphere radiation and vertical integrals over the entire atmosphere. The IFS is coupled to a soil model, the parameters of which are also designated as surface parameters,

and an ocean wave model (Malardel et al., 2016).

To realize a reliable comparison and decrease the impact of the resolution of each product, the same spatial and temporal resolutions as the kriging datasets are used. For datasets with a sub-daily temporal resolution as reanalysis data (NCEP-CFSR, ERA5), we calculated daily accumulations for 00:00-23:59 UTC like satellite and rain gauge data. The datasets with spatial
5 resolutions $< 0.25°$ were resampled to $0.25°$ using bilinear averaging, whereas those with spatial resolutions $> 0.25°$ were resampled to $0.25°$ using bi-linear interpolation (Beck et al., 2019).

1.3 Methodological approach

Based at a daily temporal and $0.25°$ spatial resolution of each dataset, a detailed analysis is done by comparing the frequencies and characteristics of the extreme events from the different products. A maximum number of definition (according to their
10 duration and intensity) are used here to highlight the differences between the products and their potential impacts. In the following section, the definitions of the methods to detect the dry and wet spells are presented.

1.3.1 Dry Spells

The definition of dry spells based on the duration of consecutive dry days. These days are detected when the daily precipitation are lower than 1 mm/day (defined to discriminate wet and dry days, (Diallo et al., 2016)). This definition is commonly used to
15 define a dry spell in Sahel and the methodology employed here is similar to the method defined in Salack et al. (2013). Then different classes of DS are defined depending their durations (DS short, DS medium, DS long, DS extreme long) described in Table 2. A second method is based on the accumulated precipitation during specific periods, and are called dry spell cumulative (DSC). Here four durations are tested, five days when the rainfall is less than 5 mm these events are called DSC5; 10 days with less than 10 mm of rainfall named DSC10; 15 days with less than 15 mm of rain named DSC10; 20 days with less than 20 mm
20 of rain for DSC20 (see Table 2). For this DSC the duration is known but the number and frequency in a season is determinant for the growth of crop yields (Sivakumar, 1992). The results presented in that study are mainly derived from only four dry indicators (DSC10, DSC20, DSl, DSxl) nevertheless, all the results from the other duration are presented in supplementary materials.

1.3.2 Wet Spells

25 We defined wet spells depending their duration and intensity. The duration categories of wet spells are chosen to correspond to the different synoptic systems causing rain in West Africa (Froidurot and Diedhiou, 2017). Moreover, four thresholds (90th, 95th, 99th, 99.5^{th} percentile of all the rainy days) are also defined. Wet spell (WS) are defined as one or consecutive rainy days (for different thresholds). WS1 99P represents a heavy precipitation day which is defined as a day with precipitation greater than the 99th percentile. WSM 99P is defined as events of at least 2 consecutive days ($<= 2$ days) of rainfall above the 99th
30 percentile. Wet spell cumulative (WSC) is defined as specific periods where cumulative rainfall is above threshold as shown

in Table 3). As for dry spell, in this study we have focused on strongest wet spells (WS1 99P, WSM 99P, WSC5 99P, WSC15 99P,) but all the results are presented in supplementary material.

2 Results and Discussions

2.1 Intra-seasonal and Spatial Variability of rainfall

5   Fig. 2 shows 13-years (1998-2010) climatology of seasonal rainfall accumulation for all the products on grids where the values derived from the kriging is considered significant (i.e. square root of the OK variance lower than 0.5 (Lloyd and Atkinson, 2001). The South-North gradient of annual rainfall total is well observed in all products with accumulation varying from 100 mm to 1200 mm. Moreover, there are no large differences between datasets. The values are even closer between TRMM and CHIRPS or TAMSAT (Fig. 2.b and Fig. 2.d). We notice some underestimations by using CMORPH and CPC over southern

10 Senegal (Fig. 2.c and Fig. 2.e) than in other datasets. Overall, the reanalysis data NCEP and ERA (Fig. 2.f and Fig. 2.g) are quite close to each other with some divergences in the western center of the country. OK and BK also show some divergences that is explained by the method of kriging used (Fig. 2.h and Fig. 2.i). Indeed, by construction, BK is more comparable to averaged values and is more in agreement with satellite results than OK. The best similar pattern of BK is found with TRMM, Precipitation Radar (PR) aboard TRMM can explain this result. However, all products further highlighted this zone of highest

15 spatial variability called "Peanut Basin" located in the center western of the country where seasonal rainfall ranging from 300 mm to 800 mm.

The seasonal evolution of the dry days, crucial for the definition of dry spells, is then compared. To do so, percentage of dry days per month for each product are shown in Fig. 3 and shows disparities. During the dry season (from November to May) all datasets record more than 80% of dry days. However, CMORPH and TAMSAT record more dry days than other datasets. At

20 the same time, OK and BK record 100% of dry days which can be explained by the funding reasons that coerce ANACIM to ensure the data gathering only during the rainy season for most of the stations. At the beginning of the season (June to July), TRMM, CPC, ERA, NCEP and OK show more dry days although there are discrepancies between datasets. While TAMSAT, CHIRPS, CMORPH and BK show less dry days. However, at the main season (August to September) TRMM, CPC, ERA and OK record more dry days than TAMSAT, CHIRPS, CMORPH, NCEP and BK. This result shows a paradox because the

25 datasets which showed low seasonal rainfall have a trend to record a low percentage of dry days (ie: more rainy days) except ERA5. Fig. 3 also illustrates a higher variability from the seasonal scale to intra-seasonal scale.

2.2 Characterization of Dry Spells

The purpose of this section is to compare the detection of different type of dry spells (depending their intensity and duration) derived from different products. For the main document, we will discuss two types of dry spells defined previously, namely

30 DSC10, DSC20, DSl, DSxl (see Table 1 for the definitions). Note that the results using the other type of dry spells are presented in supplementary material. The first comparison is done on the the yearly average occurrence of dry spells. These occurrence

are calculated for all datasets only over grid points where the kriging method is considered significant (Fig. 4). These results underscore differences between datasets on the number of DSC10, DSC20, DSl and DSxl. Among the datasets, TAMSAT and CHIRPS show slightly smaller DSC (DSC10 and DSC20) than in the other datasets. However, on DS (DSl and DSxl) BK joins CHIRPS and TAMSAT as the products that detect the lowest frequencies. Nevertheless, these detections display relative

5   similarities in between products. The main differences are the spatial spread.

The results based on DSl and DSxl show a higher variability between datasets. Indeed, TRMM, OK, CPC, CMORPH, NCEP and ERA5 provide on average 1 more dry spell events than BK, TAMSAT and CHIRPS. This result may be explained by the seasonal cycle of dry days (Fig. 3) which, except NCEP and CMORPH confirms that in products where the number of dry days is lower the number of DSl and DSxl is also lower.

10   However, divergence of datasets to agree on DS duration and intensity are mitigated on the temporal frequency of DSC and DS shown in Fig. 5. The seasonal cycle of dry spell shows slight differences between products which confirm that this events characterize false start and early cessation of season in Senegal. This gives to DSC and DS a high potential for impact on sowing and crops. This common agreement showing a minimum peak of dry spells in main season (July-August-September), illustrate also the degree of severity of DSC and DS. Indeed, the DSC20 and DSxl are the longest dry spell and therefore the

15   most intense. Despite agreement on the occurrence date of DSC and DS, we observe some differences on the number of dry spell that occur at given date. Overall, CMORPH, CHIRPS and TAMSAT show low occurrence of dry spells, in opposite, NCEP and ERA5, TRMM, CPC, OK and BK show high occurrence of DSC and DS during the main season.

In order to investigate the spatial variability of DSC10, DSC5, DSl and DSxl, Taylor diagram of all datasets (Taylor, 2001). Fig. 6 illustrates the capacity of datasets to agree on the spatial distribution of dry spell by providing the spatial correlation, the

20   standard deviation, and the root mean square deviation (RMSD) for each data set compared to OK defined as the reference. The choice of OK was motivated by the fact that the ordinary kriging method followed by a post-processing and a quantile-mapping correction is the closest to the spatial distribution of rain gauge data. We show that DSC indicators record better correlation scores than DS indicators. For all the indicators TRMM gives the best score showing the importance of radar embedded. Results from reanalysis products provide scores comparable to the observations used here.

25   Another analyze between the datasets is done with the interannual variability of the dry periods, as illustrated in Fig. 7. Overall, biases are less important with DSC than with DS. DSC20 reached its lowest level in the time series in all datasets during recovery. While it is with the DS that the biases are more important. Interannual evolution is a same in OK and BK, which is very similar with DSC are much less so with DS. This difference can be explained by the seasonal cycle of dry days (see Fig. 2) where we have 10% more dry days in OK than in BK. A similar pattern is found between datasets on the interannual

30   variability and boxplots of DS (see Fig. 4). The coherency between the OK and BK trends decrease from DSC to DS, provides confidence for inferring that DS record more disparities than DSC. Otherwise, DSl and DSxl better characterize the Sahelian specificity with the great drought (1970-2000) where DSxl has reached a very high level for all products except CPC.

2.3 Characterization of Wet Spells

2.3.1 Total rainfall accumulated in WS and WSC

In this section, the detection of different wet spells (depending their intensity and duration) derived from different datasets is assessed and compared. In the main document, four types of wet spells using the 99th percentile of rainfall above the depth of
5 wet day defined previously, namely WS1 99P, WSM 99P, WSC5 99P, WSC15 99P (see Table 2) are discussed. Note that as on dry spell, the results using other type of wet spells are presented in supplementary material. First, the yearly average occurrence of wet spells calculated for all the products only over grid points where the kriging method is considered significant (see Fig. 8) is analyzed. For the less intense events (WS1 99P and WSC5 99P), we note an overall good agreement of the products with, as expected, a maximum mid of August when the monsoon is well established. The only significant differences are found with
10 CHIRPS that tends to underestimate the occurrence of the events all along the year and CMORPH, that underestimate the peak but also with a delay of about 2 weeks. When looking most intense events (WSM 99P), the differences are the largest. ERA5 clearly overestimate the occurrence (almost twice larger than the other products).

Conversely to dry spells the contrasts are more marked in wet spells, illustrating the more complex event to characterize. Overall, Fig. 9 shows three different groups of datasets. TRMM and OK provide on average accumulation of 70 mm for
15 the WS1 99P, 140 mm for the WSM 99P, 150mm for the WSC5 99P and 300 mm for the WSC15 99P. Although, average accumulation of OK are slightly greater than in TRMM on the 4 wet indicators. BK, CMORPH, CPC, NCEP and ERA5, provides smaller accumulations than the first group. Indeed, the average accumulation of WS1 99P is around 45 mm, 90 mm for WSM 90P, 100 mm for WSC5 99P and around 200 mm for WSC15 99P. Finally, TAMSAT and CHIRPS give the lowest accumulations of all products with around 30 mm for WS1 99P, around 50 mm for WSM 99P and WSC5 99P and 150 mm
20 for WSC15 99P. Note that TAMSAT accumulations are each time slightly lower than in CHIRPS. The novelty of this section is that datasets showing the most number dry days (see Fig. 2) provide the highest wet spell accumulation. While the datasets providing the least number of dry days (ie: more rainy days) record smallest wet spell accumulation. This result confirms that the radar on the TRMM satellite may be explain the agreement between TRMM and OK on the detection of wet indicators intensity and its difference with other datasets.

25 In order to better identify the reasons of these differences, the logarithmic distribution of daily rainfall over the consensual period from 1998 to 2010 is calculated (Fig. 10). This distribution allows to see tipping points on daily rainfall. Daily rainfall less than 25mm are more frequent on TAMSAT and CHIRPS. These two products record the most rainy days in main season (Fig. 2). TRMM, OK, BK, CPC, CMORPH and CHIRPS show high frequency of 25 mm - 30 mm unlike TAMSAT, ERA5 and NCEP showing lower frequency of these intensities. The differences increase with daily rainfall between 30 and 60 mm,
30 and beyond 60 mm. TRMM produces the largest rainfall events, a bit larger than a group of OK, BK, CPC, ERA5 and NCEP. Finally, TAMSAT, CHIRPS and CMORPH are associated with the lowest frequency of these extreme events. This characterization is essential to understand the capacity of datasets to detect extreme rainfall and show a large underestimation of these 3 products.

The Taylor diagram provided in Fig. 11 is similarly constructed to the one of the dry spells. It provides spatial correlations, standard deviations and RMSD for each data set compared to OK kept as a reference. It is interesting to note that the scores are worse compared to the dry spells showing the bigger complexity to assess wet than dry spells. This is observed with the decrease of correlation, the significant increase of standard deviation and RMSD. The most complex assessment of events

5   seems to be WSM99P, which is the rarest. CHIRPS and CMORPH seem to be incapable to assess these events compared to the events detected by using OK. It is worth to note the strong consistency of the datasets to assess the two WSC and WS1. CMORPH is the only product with significant lower correlation and larger RMSD compared to the others. This shape could be explained by the correct representation of a fraction of the events in all the products. This fraction explains the non-perfect correlation compared to the OK (between 0.6 to 0.8) and a RMSD around 3.

10   Finally, to analyze the recent trend of these extreme events, Fig. 12 provides the evolution of the number of each type of wet spells per year. The results are in line with the recent study of Taylor et al. (2017) suggesting that the Mesoscale Convective Systems (MCSs) responsible for extreme rainfall in the Sahel have tended to increase their vertical development, favoring the convergence of humidity and producing exceptional cumulative rainfall. Since the beginning of the 2000s, all datasets show an increase of these indicators. This increase is more significant on the WSC5 99P and WSC15 99P where several products

15   reached their highest level. There is a strong similarity between OK and BK with a significant increase of all the indicators. Overall, the explanation of these increases may be the intensification of the hydrological cycle that accompanies the recovery in Sahel.

3   Conclusions

In this work, extreme rainfall deficits derived from 5 satellite products (TRMM, TAMSAT, CMORPH, CPC, CHIRPS) and

20   2 re-analysis model outputs (NCEP and ERA5) have been assessed and compared to 2 kriging methods (OK and BK) spatially interpolated rain gauge data over Senegal. Two types of kriging technical have been employed to test different type of interpolation and to assess the uncertainties of these products. All the used products are upgraded to the spatial resolution of $0.25° \times 0.25°$. Then, different definition of wet and dry spell are used to detect and compare their spatial and temporal distributions over Senegal. The climatology of all products are relatively similar with a strong gradient South-North. In addition

25   the products also shows an agreement on the high spatial variability in the peanut basin in the western center of the country. Despite these similarities, some disparities between products are observed South of the country. Four datasets CMORPH, CPC, ERA5 and NCEP provide low cumulative volumes in the South compared to the other 5 datasets, TRMM, TAMSAT, CHIRPS, OK and BK which show strong accumulations in the South of the country. The discrepancies are stronger on the seasonal cycle of dry days where the products are divided into 4 groups. A first group consisting of TRMM and ERA5 where the percentage of dry days exceeds 50%. The second group consists of CPC and OK between 50 to 45% of dry days. The third group is the most representative with 4 data products NCEP, CMORPH, CHIRPS and TAMSAT where the percentage of dry days is between 45 to 40%. Finally the fourth group consists of a single data product in this case BK with about 30% of dry days. The complexity of the detection of four indicators of dry spells DSC10, DSC20, DSl and DSxl by all datasets are then compared.

The occurrence of the DSC10 and DSC20 show more coherence than for DSl and DSxl. On these divergences 2 groups stand out, the first group consists of six TRMM, OK, CPC, CMORPH, NCEP and ERA5 products. These products give on average 1 more dry spell events than the second group consisting of three products BK, TAMSAT and CHIRPS. The greatest performance of datasets is found in their ability to represent the seasonal cycle of dry spells. All products show common agreement with a minimum peak of dry spells in main season. Overall, all datasets agree that these events characterize mainly false starts and early cessation of rainy season.

The detection of wet spells is more contrasted with larger difference between datasets than for the DS. TRMM and OK produce the largest amount of rainfall. These products give on average accumulation of 70 mm for the WS1 99P, 140 mm for the WSM 99P, 150 mm for the WSC5 99P and 300 mm for the WSC15 99P. Note that the average of OK are a little more important than in TRMM on the 4 indicators. The second group is composed by BK, CMORPH, CPC, NCEP and ERA5, this group provides smaller accumulations than group 1. Indeed, the average accumulation of WS1 99P is around 45 mm, 90 mm for WSM 90P, 100 mm for WSC5 99P and around 200 mm for WSC15 99P. Finally, the third group consists by TAMSAT and CHIRPS group provides the lowest accumulations of all products with around 30 mm for WS1 99P, around 50mm for WSM 99P and WSC5 99P and 150 mm for WSC15 99P. The radar on TRMM can be the main explanation of the similarity between TRMM and OK. WSM 99P shows smaller spatial correlations than the WSC5 99P, WSC15 99P and WSM 99P. an significant increase is found on the WSC5 99P and WSC15 99P where several products reached their highest level except NCEP, CPC and CHIRPS. A strong similarity between OK and BK with a significant increase of all the indicators is found.

This study shows that despite the general agreement about the seasonal rainfall, there is a large uncertainty associated with the assessment of extreme deficit and exceedance of rainfall at intra-seasonal timescale. This study allows to validate the most robust datasets over Senegal that could be extrapolated to all of West Africa. This is crucial in order to monitor, to predict and to determine the potential socio-economic impact of these extreme wet and dry spells.

Author contributions. NF made the analysis and, NF, CL, MD GP discuss the results and wrote the paper. GP supports this study for the krigging methods. AG advises and provides scientific recommendations

Competing interests. The authors declare that they have no conflict of interest.

References

Alhassane, A., Salack, S., Ly, M., Lona, I., Traore, S., and Sarr, B.: Evolution of agro-climatic risks related to the recent trends of the rainfall regime over the Sudano-Sahelian region of West Africa, Science et changements planétaires / Sécheresse, 24, 282–93, https://doi.org/10.1684/sec.2013.0400, 2013.

5 Ali, A., Amani, A., Diedhiou, A., and Lebel, T.: Rainfall Estimation in the Sahel. Part II: Evaluation of Rain Gauge Networks in the CILSS Countries and Objective Intercomparison of Rainfall Products, Journal of Applied Meteorology - J APPL METEOROL, 44, 1707–1722, https://doi.org/10.1175/JAM2305.1, 2005.

ARC: Risk Pool I – 2014/2015, http://www.africanriskcapacity.org/2016/10/30/risk-pool-i/, 2014.

Beck, H., Pan, M., Roy, T., Weedon, G., Pappenberger, F., van Dijk, A., Huffman, G., F. Adler, R., and Wood, E.: Daily evaluation
10 of 26 precipitation datasets using Stage-IV gauge-radar data for the CONUS, Hydrology and Earth System Sciences, 23, 207–224, https://doi.org/10.5194/hess-23-207-2019, 2019.

Berthou, S., Rowell, D. P., Kendon, E. J., Roberts, M. J., Stratton, R. A., Crook, J. A., and Wilcox, C.: Improved climatological precipitation characteristics over West Africa at convection-permitting scales, Climate Dynamics, https://doi.org/10.1007/s00382-019-04759-4, 2019.

Creutin, J. and Obled, C.: Objective Analyses and Mapping Techniques for Rainfall Fields: An Objective Comparison, Water Resources
15 Research - WATER RESOUR RES, 18, 413–431, https://doi.org/10.1029/WR018i002p00413, 1982.

Descroix, L., Diongue Niang, A., Panthou, G., Bodian, A., Sane, Y., Dacosta, H., Malam Abdou, M., Vandervaere, J.-P., and Quantin, G.: Évolution récente de la pluviométrie en Afrique de l'ouest à travers deux régions : la Sénégambie et le Bassin du Niger Moyen, Climatologie, 12, 25–43, https://doi.org/10.4267/climatologie.1105, 2016.

Diallo, I., Giorgi, F., Deme, A., Tall, M., Mariotti, L., and Gaye, A.: Projected changes of summer monsoon extremes and hydroclimatic
20 regimes over West Africa for the twenty-first century, Climate Dynamics, 47, https://doi.org/10.1007/s00382-016-3052-4, 2016.

Dieng, O., Roucou, P., and Louvet, S.: Variabilité intra-saisonnière des précipitations au Sénégal (1951-1996), 2008.

Dinku, T., Ceccato, P., Grover-Kopec, E., Lemma, M., Connor, S. J., and Ropelewski, C. F.: Validation of satellite rainfall products over East Africa's complex topography, International Journal of Remote Sensing, 28, 1503–1526, https://doi.org/10.1080/01431160600954688, https://doi.org/10.1080/01431160600954688, 2007.

25 Dione, C., Lothon, M., Daouda, B., Campistron, B., Couvreux, F., Guichard, F., and Sall, S. M.: Phenomenology of Sahelian convection observed in Niamey during the early monsoon, Quarterly Journal of the Royal Meteorological Society, 140, https://doi.org/10.1002/qj.2149, 2014.

Ebert, E., Janowiak, J., and Kidd, C.: Comparison of Near-Real-Time Precipitation Estimates From Satellite Observations, Bulletin of The American Meteorological Society - BULL AMER METEOROL SOC, 88, https://doi.org/10.1175/BAMS-88-1-47, 2007.

30 Ferraro, R.: SSM/I derived global rainfall estimates for climatological applications, Journal of Geophysical Research, 1021, 16 715–16 736, https://doi.org/10.1029/97JD01210, 1997.

Ferraro, R. and Li, Q.: Detailed analysis of the error associated with the rainfall retrieved by the NOAA/NESDIS Special Sensor Microwave/Imager algorithm 2. Rainfall over land, Journal of Geophysical Research, 107, https://doi.org/10.1029/2001JD001172, 2002.

Froidurot, S. and Diedhiou, A.: Characteristics of Wet and Dry Spells in the West African Monsoon System, Atmospheric Science Letters,
35 18, https://doi.org/10.1002/asl.734, 2017.

Funk, C., Peterson, P., Landsfeld, M., Pedreros, D., Verdin, J., Shukla, S., Husak, G., Rowland, J., Harrison, L., Hoell, A., and Michaelsen, J.: The climate hazards infrared precipitation with stations - A new environmental record for monitoring extremes, Scientific Data, 2, 150 066, https://doi.org/10.1038/sdata.2015.66, 2015.

Giorgi, F., Im, E.-S., Coppola, E., Diffenbaugh, N. S., Gao, X. J., Mariotti, L., and Shi, Y.: Higher Hydroclimatic Intensity with Global Warming, Journal of Climate, 24, 5309–5324, https://doi.org/10.1175/2011JCLI3979.1, 2011.

Goovaerts, P.: Geostatistical Approaches for Incorporating Elevation Into the Spatial Interpolation of Rainfall, Journal of Hydrology, 228, 113–129, https://doi.org/10.1007/s00703-005-0116-0, 2000.

Grimes, D., Pardo-Iguzquiza, E., and Bonifacio, R.: Optimal Areal Rainfall Estimation Using Raingauges and Satellite Data, Journal of Hydrology, 222, 93–108, https://doi.org/10.1016/S0022-1694(99)00092-X, 1999.

Held, I. M. and Soden, B.: Robust Response of the Hydrological Cycle to Global Warming, AGU Fall Meeting Abstracts, 19, https://doi.org/10.1175/JCLI3990.1, 2008.

Huffman, G., Adler, R., Bolvin, D., Gu, G., Nelkin, E., Bowman, K., Stocker, E., and Wolff, D.: The TRMM multi-satellite precipitation analysis: Quasi-global, multi-year, combined-sensor precipitation estimates at fine scale, J. Hydrometeor., 8, 28–55, 2007.

Janowiak, J., Joyce, R., and Yarosh, Y.: A Real-Time Global Half-Hourly Pixel-Resolution Infrared Dataset and Its Applications, Bulletin of the American Meteorological Society, 82, https://doi.org/10.1175/1520-0477(2001)082<0205:ARTGHH>2.3.CO;2, 2001.

Jobard, I., Berges, J., Chopin, F., and Roca, R.: EPSAT-SG: A satellite method for precipitation estimation; its concepts and implementation for the AMMA experiment, Annales Geophysicae, 28, 289–308, 2010.

Joyce, R., Janowiak, J., Arkin, P., and Xie, P.: CMORPH: A Method That Produces Global Precipitation Estimates From Passive Microwave and Infrared Data at High Spatial and Temporal Resolution, Journal of Hydrometeorology - J HYDROMETEOROL, 5, https://doi.org/10.1175/1525-7541(2004)005<0487:CAMTPG>2.0.CO;2, 2004.

Kendon, E. J., Stratton, R. A., Marsham, J. H., Berthou, S., and Rowell, David P.and Senior, C. A.: Enhanced future changes in wet and dry extremes over Africa at convection-permitting scale, Nature Communications, 10, 2041–1723, https://doi.org/https://doi.org/10.1038/s41467-019-09776-9, 2019.

Knapp, K. R., Ansari, S., Bain, C. L., Bourassa, M. A., Dickinson, M. J., Funk, C., Helms, C., Hennon, C. C., Holmes, C., Huffman, G., Kossin, J. P., Lee, H. T., Loew, A., and Magnusdottir, G.: Globally Gridded Satellite Observations for Climate Studies, Bulletin of the American Meteorological Society, 92, 893–907, https://doi.org/10.1175/1525-7541(2004)005<0487:CAMTPG>2.0.CO;2, 2011.

Kummerow, C., Barnes, W., Kozu, T., Shiue, J., and Simpson, J.: The Tropical Rainfall Measuring Mission (TRMM) sensor package, Journal of Atmospheric and Oceanic Technology - J ATMOS OCEAN TECHNOL, 15, 809–817, https://doi.org/10.1175/1520-0426(1998)015<0809:TTRMMT>2.0.CO;2, 1998.

Lafore, J.-P., Beucher, F., Peyrillé, P., Diongue-Niang, A., Chapelon, N., Bouniol, D., Caniaux, G., Favot, F., Ferry, F., Guichard, F., Poan, D., Roehrig, R., and Vischel, T.: A multi-scale analysis of the extreme rain event of Ouagadougou in 2009, Quarterly Journal of the Royal Meteorological Society, https://doi.org/10.1002/qj.3165, 2017.

Le Barbé, L., Lebel, T., and Tapsoba, D.: Rainfall Variability in West Africa during the Years 1950–90, Journal of Climate, 15, 187–202, https://doi.org/10.1175/1520-0442(2002)015<0187:RVIWAD>2.0.CO;2, 2002.

Lebel, T. and Ali, A.: Recent trends in the Central and Western Sahel rainfall regime (1990–2007), Journal of Hydrology, 375, 52–64, https://doi.org/10.1016/j.jhydrol.2008.11.030, 2009.

Lloyd, C. and Atkinson, P.: Assessing Uncertainty in Estimates with Ordinary and Indicator Kriging, Computers and Geosciences - COMPUT GEOSCI, 27, 929–937, https://doi.org/10.1016/S0098-3004(00)00132-1, 2001.

Maidment, R., Grimes, D., Allan, R., Greatrex, H., Rojas, O., and Leo, O.: Evaluation of satellite-based and model re-analysis rainfall estimates for Uganda, Meteorological Applications, 20, https://doi.org/10.1002/met.1283, 2013.

Maidment, R., Grimes, D., Black, E., Tarnavsky, E., Young, M., Greatrex, H., Allan, R., Stein, T., Nkonde, E., Senkunda, S., and Uribe, E.: A new, long-term daily satellite-based rainfall dataset for operational monitoring in Africa, Scientific Data, 4,
5   https://doi.org/10.1038/sdata.2017.63, 2017.

Malardel, S., Wedi, N., Deconinck, W., Diamantakis, M., Kühnlein, C., Mozdzynski, G., Hamrud, M., and Smolarkiewicz, P.: A new grid for the IFS, ECMWF Newsletter, 146, 23–28, 2016.

Nesbitt, S. W., Cifelli, R., and Rutledge, S. A.: Storm Morphology and Rainfall Characteristics of TRMM Precipitation Features, Monthly Weather Review, 134, 2702–2721, https://doi.org/10.1175/MWR3200.1, 2006.

10   Nicholson, S.: The West African Sahel: A Review of Recent Studies on the Rainfall Regime and Its Interannual Variability, ISRN Meteorology, 2013, https://doi.org/10.1155/2013/453521, 2013.

Nicholson, S., Fink, A., and Funk, C.: Assessing recovery and change in West Africa's rainfall regime from a 161-year record, International Journal of Climatology, 38, 3770–3786, https://doi.org/10.1002/joc.5530, 2018.

Panthou, G., Vischel, T., and Lebel, T.: Recent trends in the regime of extreme rainfall in the Central Sahel, International Journal of Clima-
15   tology, 34, https://doi.org/10.1002/joc.3984, 2014.

Panthou, G., Lebel, T., Vischel, T., Quantin, G., Sane, Y., Abdramane, B., Ndiaye, O., Diongue Niang, A., and Diopkane, M.: Rainfall intensification in tropical semi-arid regions: The Sahelian case, Environmental Research Letters, 13, https://doi.org/10.1088/1748-9326/aac334, 2018.

Sagna, P., Ndiaye, O., Diop, C., Diongue-Niang, A., and Corneille, S.: Are recent climate variations observed in Senegal in conformity with
20   the descriptions given by the IPCC scenarios?, Atmospheric Pollution, 227, 2015.

Saha, S., Moorthi, S., Pan, H.-L., Wu, X., Wang, J., Nadiga, S., Tripp, P., Kistler, R., Woollen, J., Behringer, D., Liu, H., Stokes, D., Grumbine, R., Gayno, G., Wang, J., Hou, Y.-T., Chuang, H.-Y., Juang, H.-M., Sela, J., and Goldberg, M.: The NCEP climate forecast system reanalysis, Bulletin of The American Meteorological Society - BULL AMER METEOROL SOC, 91, https://doi.org/10.1175/2010BAMS3001.1, 2010.

25   Salack, S., Giannini, A., Diakhate, M., Gaye, A., and Muller, B.: Oceanic influence on the sub-seasonal to interannual timing and frequency of extreme dry spells over the West African Sahel, Climate Dynamics, 42, https://doi.org/10.1007/s00382-013-1673-4, 2013.

Salack, S., Klein, C., Giannini, A., Sarr, B., Worou, N., Belko, N., Bliefernicht, J., and Kunstman, H.: Global warming induced hybrid rainy seasons in the Sahel, Environmental Research Letters, 11, 104 008, https://doi.org/10.1088/1748-9326/11/10/104008, 2016.

Sane, Y., Panthou, G., Bodian, A., Vischel, T., Lebel, T., Dacosta, H., Quantin, G., Wilcox, C., Ndiaye, O., Diongue Niang, A., and Diop Kane,
30   M.: Intensity-Duration-Frequency (IDF) rainfall curves in Senegal, Natural Hazards and Earth System Sciences Discussions, 18, 1–30, https://doi.org/10.5194/nhess-18-1849-2018, 2018.

Sivakumar, M.: Empirical analysis of dry spells for agricultural applications in west Africa, Journal of Climate, 24, 532–539, 1992.

Tabios, G. and Salas, J.: A Comparative Analysis of Techniques for Spatial Interpolation of Precipitation, Journal of the American Water Resources Association, 21, 365–380, https://doi.org/doi/10.1111/j.1752-1688.1985.tb00147.x, 1985.

35   Tarnavsky, E., Grimes, D., Maidment, R., Black, E., Allan, R., Stringer, M., Chadwick, R., and Kayitakire, F.: Extension of the TAMSAT Satellite-Based Rainfall Monitoring over Africa and from 1983 to Present, Journal of Applied Meteorology and Climatology, 53, 2805–2822, https://doi.org/10.1175/JAMC-D-14-0016.1, 2014.

Taylor, C., Belušić, D., Guichard, F., Parker, D., Vischel, T., Bock, O., P. Harris, P., Janicot, S., Klein, C., and Panthou, G.: Frequency of extreme Sahelian storms tripled since 1982 in satellite observations, Nature, 544, 475–478, https://doi.org/10.1038/nature22069, 2017.

Taylor, K. E.: Summarizing multiple aspects of model performance in a single diagram, Journal of Geophysical Research, 106, 7183–7192, https://doi.org/10.1029/2000JD900719, 2001.

5 Thorne, V., Coakeley, P., Grimes, D., and Dugdale, G.: Comparison of TAMSAT and CPC Rainfall Estimates with rainfall, for southern Africa, International Journal of Remote Sensing, 22, 1951–1974, https://doi.org/10.1080/01431160118816, 2001.

Trenberth, K. E.: Attribution of Climate Variations and Trends to Human Influences and Natural Variability, Wiley Interdisciplinary Reviews: Climate Change, 2, 925 – 930, https://doi.org/10.1002/wcc.142, 2011.

Trenberth, K. E., Dai, A., M. Rasmussen, R., and Parsons, D.: The Changing Character of Precipitation, Bull. Amer. Meteor. Soc., 84, 10 1205–1217, https://doi.org/10.1175/BAMS-84-9-1205, 2003.

Washington, R., Harrison, M., Conway, D., Black, E., Challinor, A., Grimes, D., Jones, R., Morse, A., Kay, G., and Todd, M.: African Climate Change: Taking the Shorter Route, Bulletin of the American Meteorological Society, 87, https://doi.org/10.1175/BAMS-87-10-1355, 2006.

WFP: WFP Senegal Country Brief, January 2018, 2018.

15 Wilcox, C., Vischel, T., Panthou, G., Bodian, A., Blanchet, J., Descroix, L., Quantin, G., Cassé, C., Tanimoun, B., and Kone, S.: Trends in hydrological extremes in the Senegal and Niger Rivers, Journal of Hydrology, 566, https://doi.org/10.1016/j.jhydrol.2018.07.063, 2018.

Xie, P., Joyce, R., Wu, S., Yoo, S.-H., Yarosh, Y., Sun, F., and Lin, R.: Reprocessed, Bias-Corrected CMORPH Global High-Resolution Precipitation Estimates from 1998, Journal of Hydrometeorology, 18, https://doi.org/10.1175/JHM-D-16-0168.1, 2017.

Yeni, F. and Alpas, H.: Vulnerability of global food production to extreme climatic events, Food Research International, 96, 20 https://doi.org/10.1016/j.foodres.2017.03.020, 2017.

Zeweldi, D. and Gebremichael, M.: Evaluation of CMORPH Precipitation Products at Fine Space-Time Scales, Journal of Hydrometeorology - J HYDROMETEOROL, 10, https://doi.org/10.1175/2008JHM1041.1, 2009.
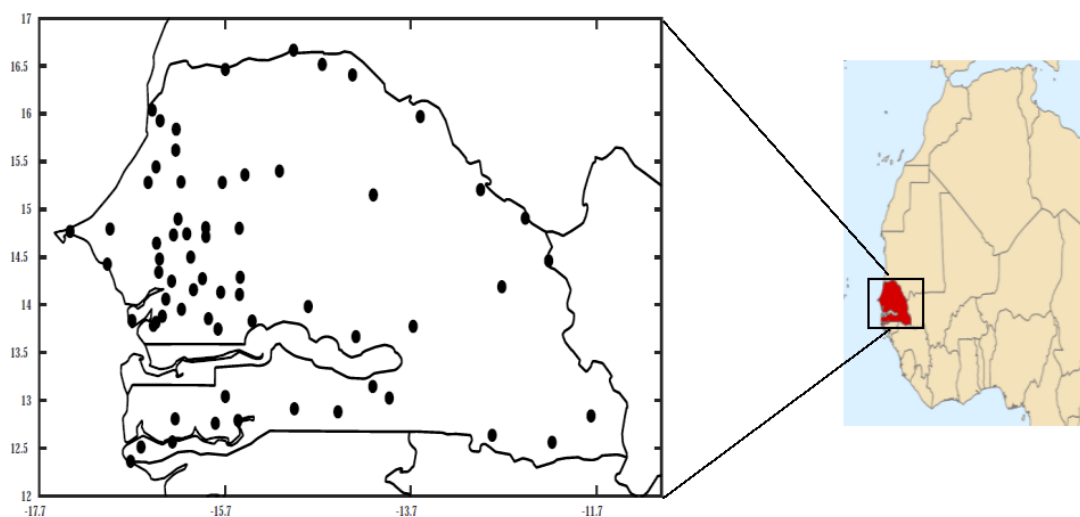
Figure 1. Map of Senegal and of West-Africa (inset). The black dots denote 65 rain gauges of ANACIM used for this study
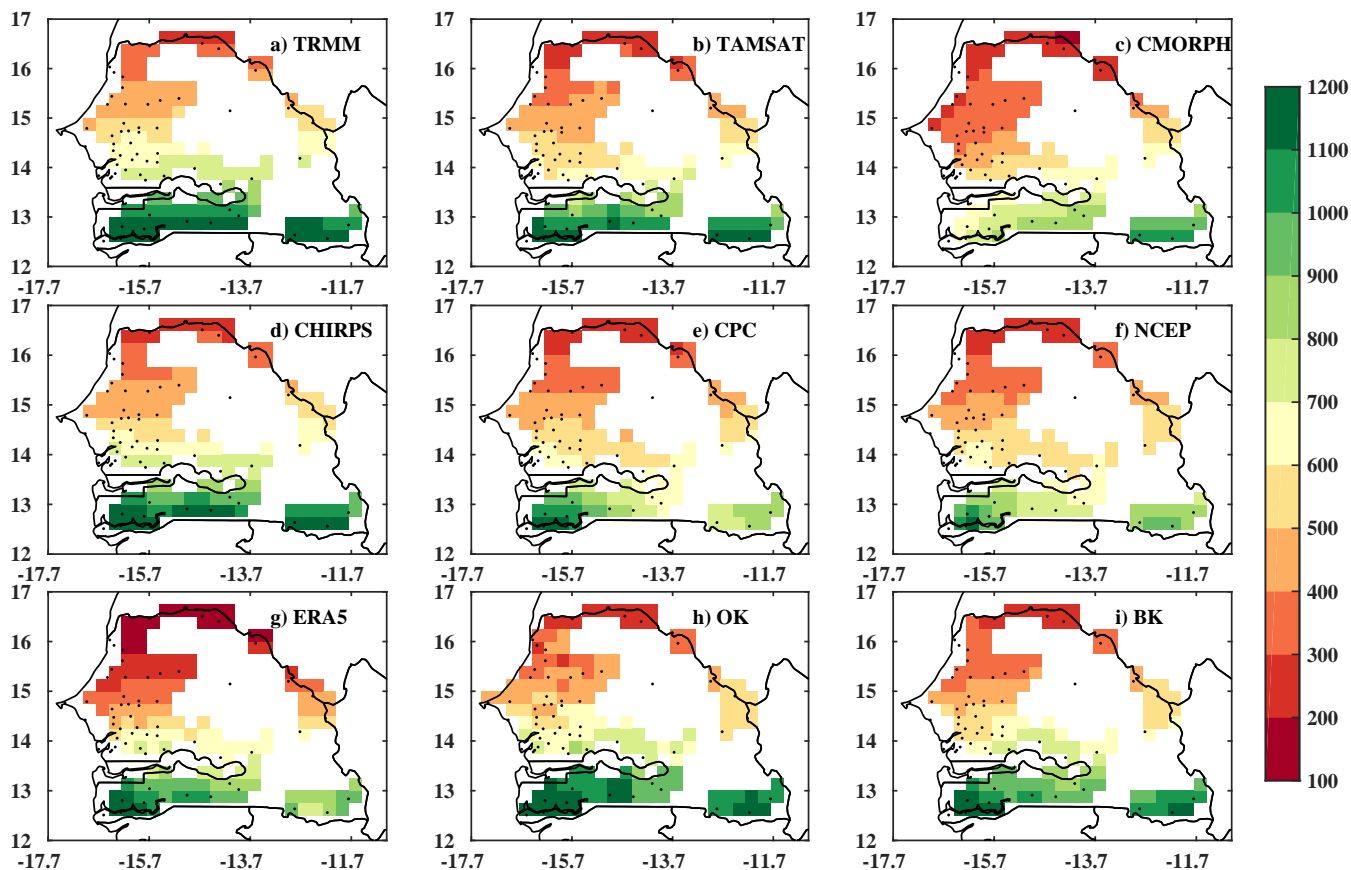
Figure 2. Spatial distribution of the climatological yearly rainfall (1998-2010, in mm): using a) TRMM b) TAMSAT c) CMORPH d) CHIRPS, e) CPC, f) NCEP g) ERA5 h) OK i) BK. The black dots represent the stations used. Details on the datasets are provided in Table 1
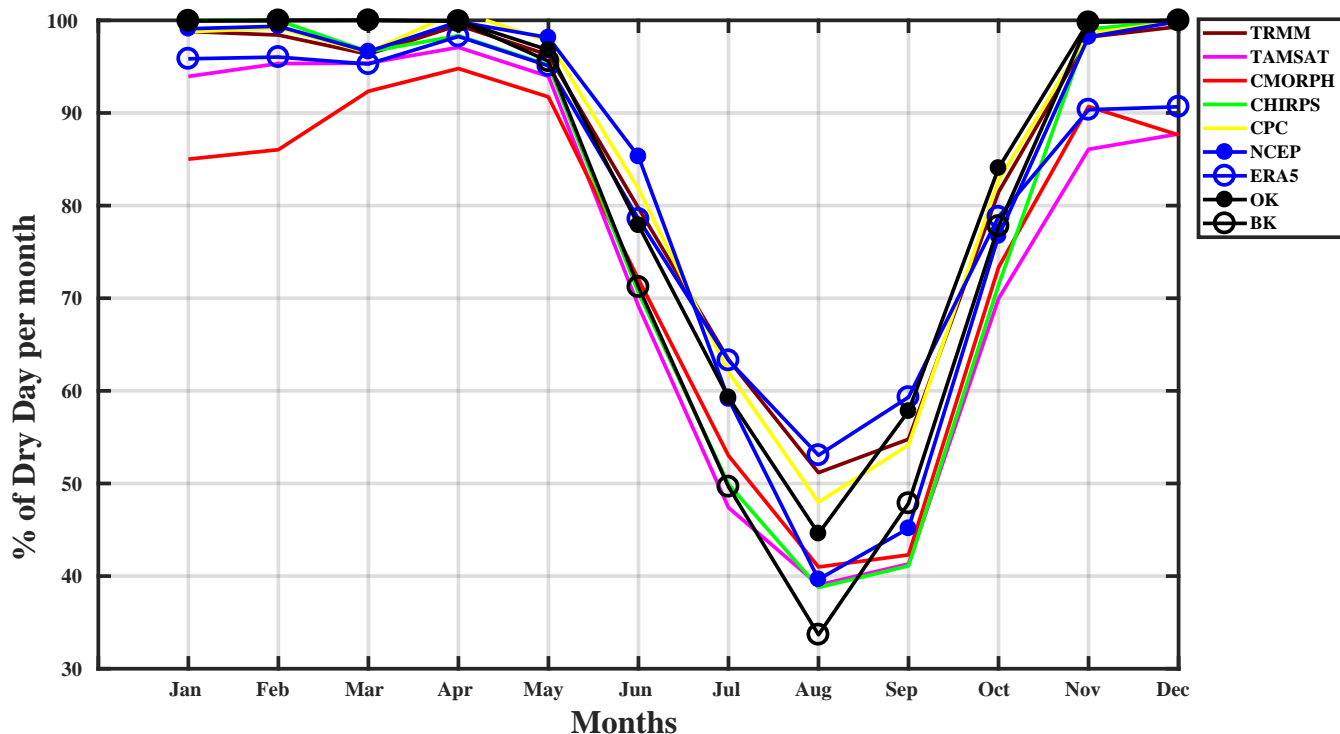
Figure 3. Seasonal cycle of the climatological (1998-2010) distribution of dry days for : TRMM, TAMSAT, CMORPH, CHIRPS, CPC, NCEP, ERA5, BK, OK. The black dots represent the stations used. Details on the datasets are provided in Table 1
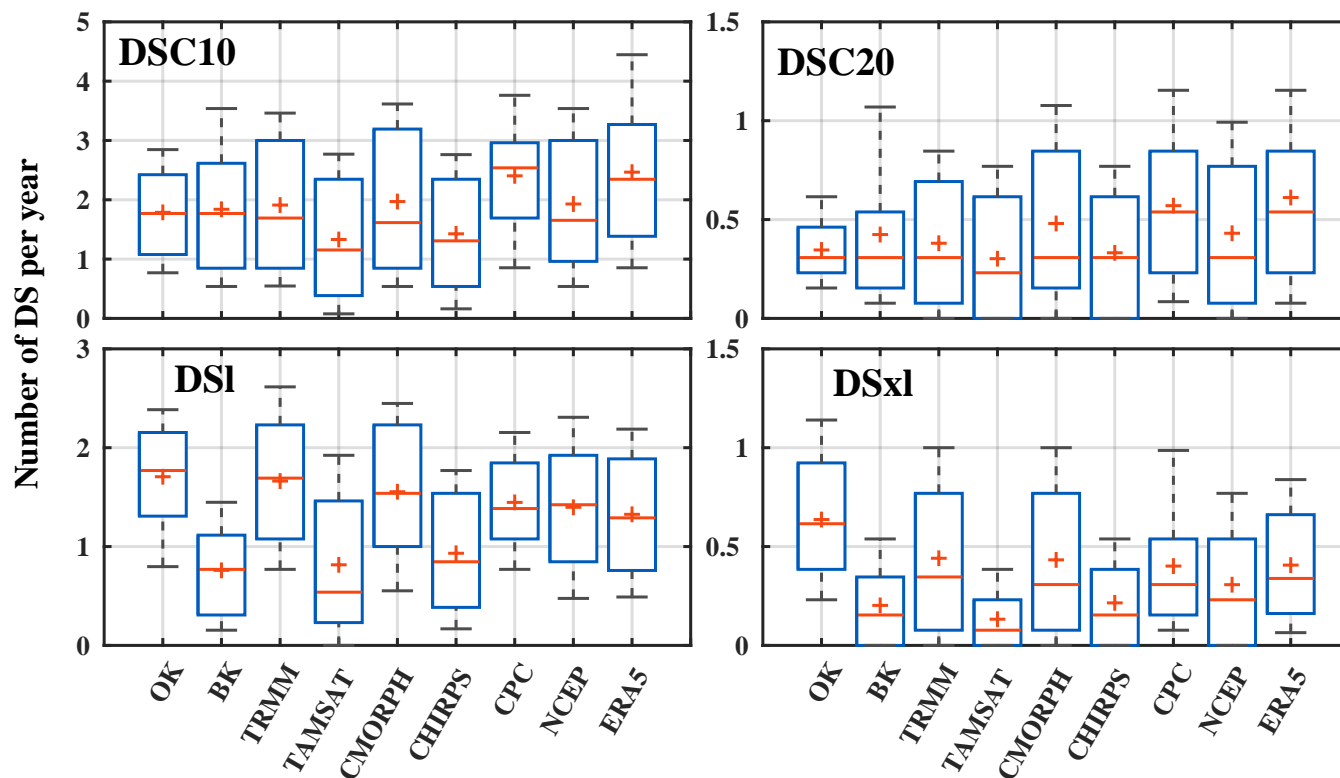
Figure 4. Total climatological (1998-2010) distribution of the number of DSC10, DSC20, DSl and DSxl for datasets: TRMM, TAMSAT, CMORPH, CHIRPS, CPC, NCEP, ERA5, BK, OK. The + represent the mean value, the − represent the median value, the box represents the 25th and 75th percentile values, and the "whiskers" represent the extreme values. Details on the datasets are provided in Table 1
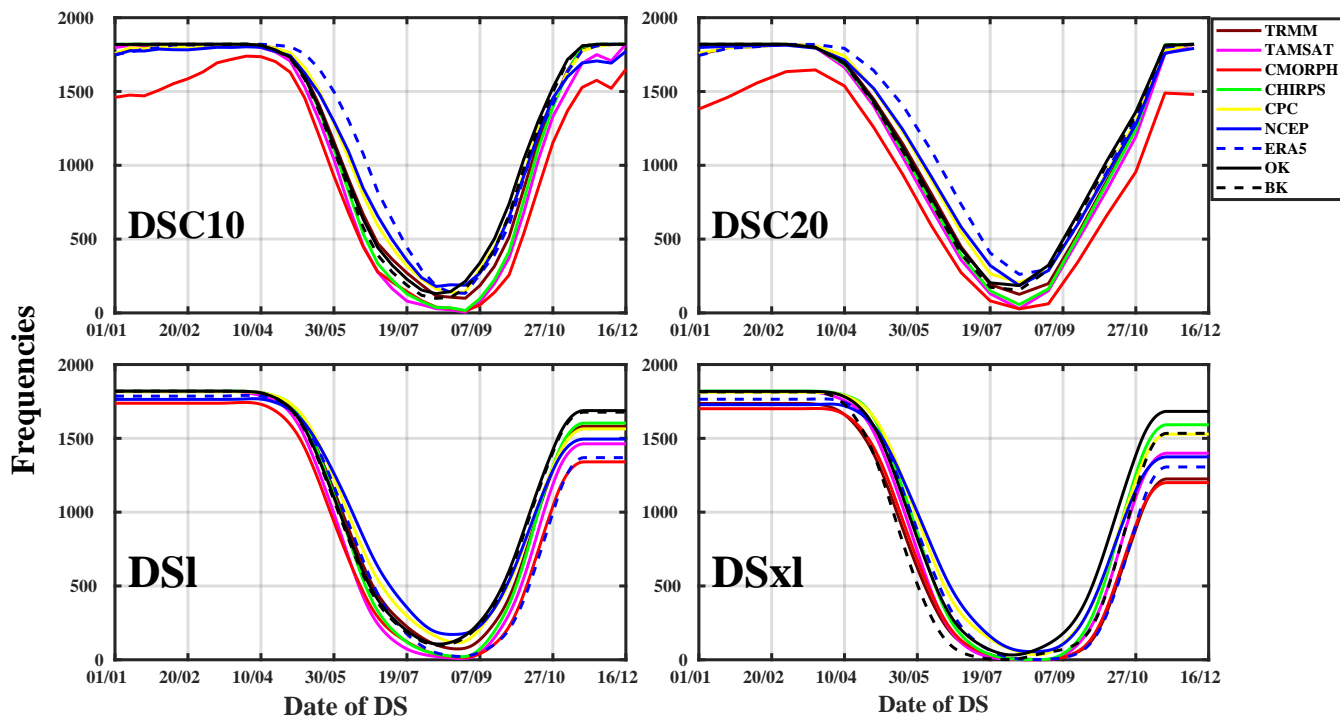
Figure 5. Climatological (1998-2010) distribution of the seasonal distribution of number of DSC5, DSC15, DSs and DSm for : TRMM, TAMSAT, CMORPH, CHIRPS, CPC, NCEP, ERA5, BK, OK. Details on the datasets are provided in Table 1.
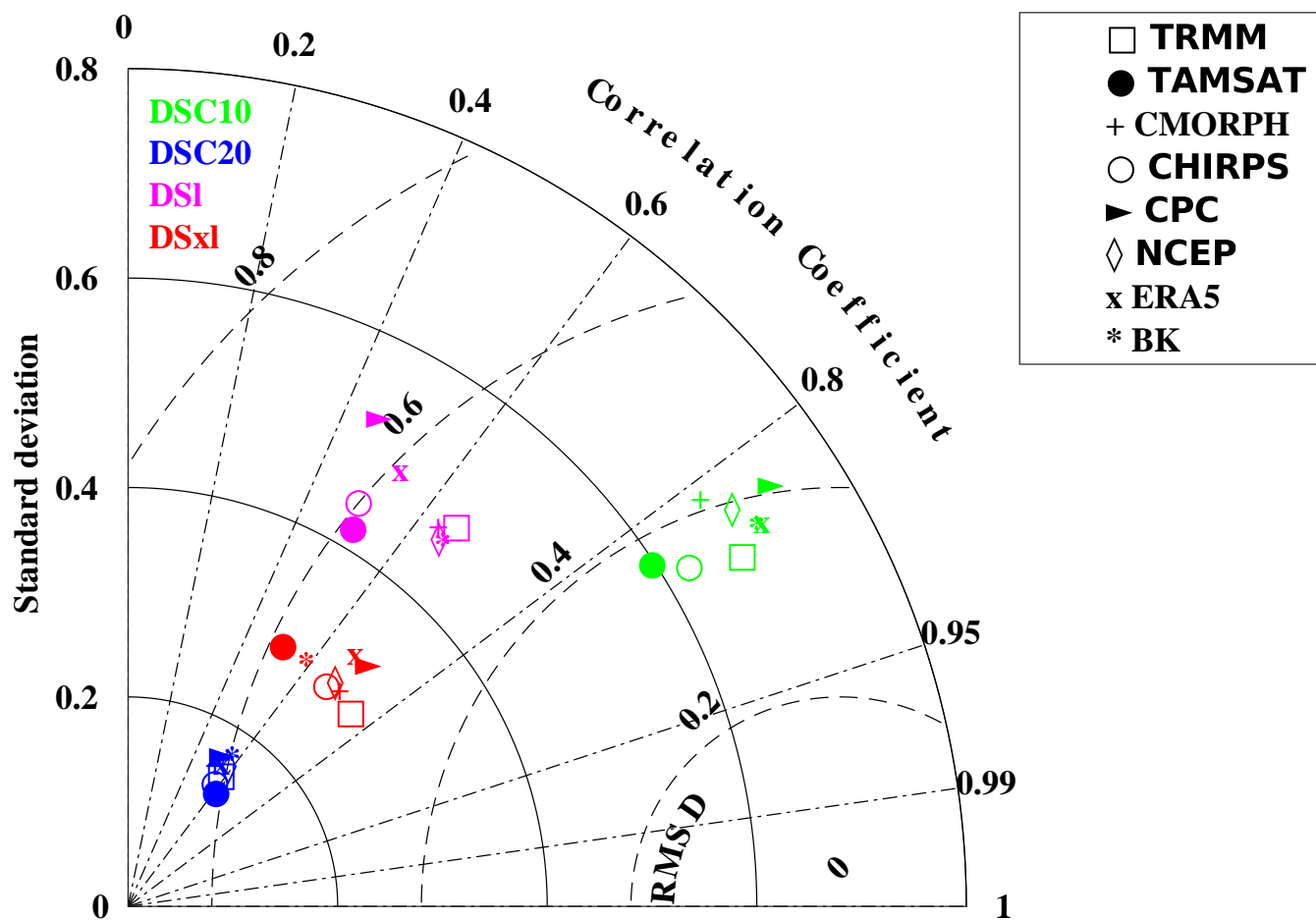
Figure 6. Taylor Diagram of the spatial distribution of number of DSC10, DSC20, DSl and DSxl for : TRMM, TAMSAT, CMORPH, CHIRPS, CPC, NCEP, ERA5, BK. OK product is considered as reference. Details on the datasets are provided in Table 1
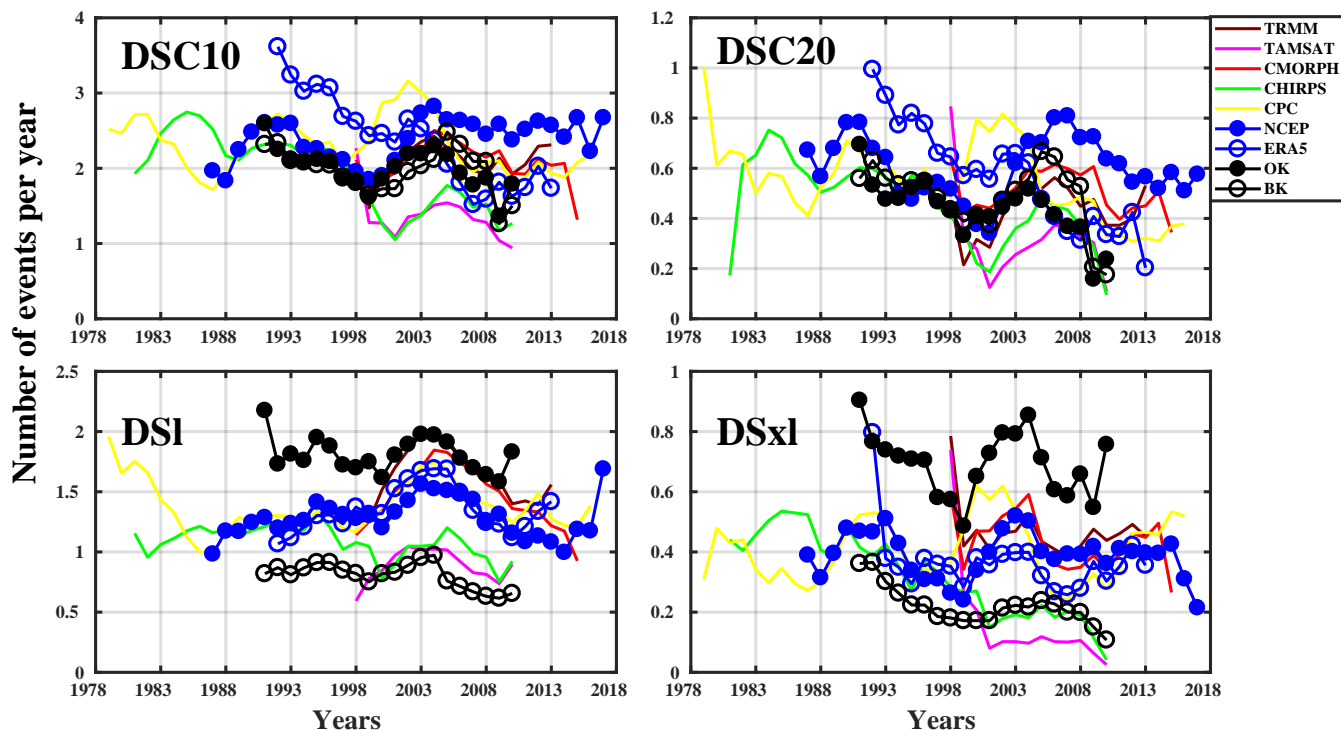
Figure 7. Interannual variability of the number of DSC10, DSC20, DSl and DSxl for : TRMM (1998-2013), TAMSAT(1998-2010), CMORPH (1998-2015), CHIRPS (1981-2010), CPC (1979-2016), NCEP (1992-2013), ERA5 (1987-2017), BK (1991-2010), OK (1991-2010). Details on the datasets are provided in Table 1
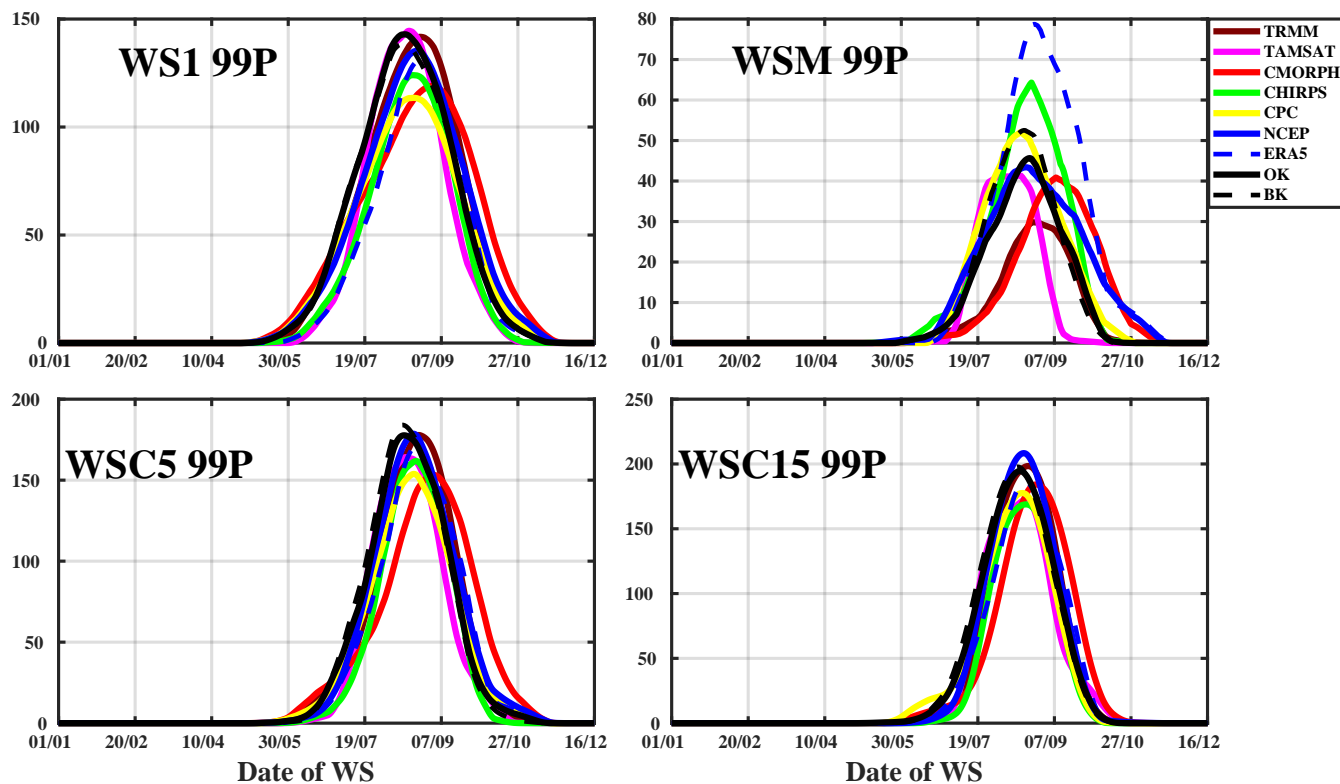
Figure 8. Seasonal cycle of the number of WS1, WSM, WSC5 and WSC15 (99th) percentiles averaged for the period 1998-2010, for : TRMM, TAMSAT, CMORPH, CHIRPS, CPC, NCEP, ERA5, BK, OK. Details on the datasets are provided in Table 1
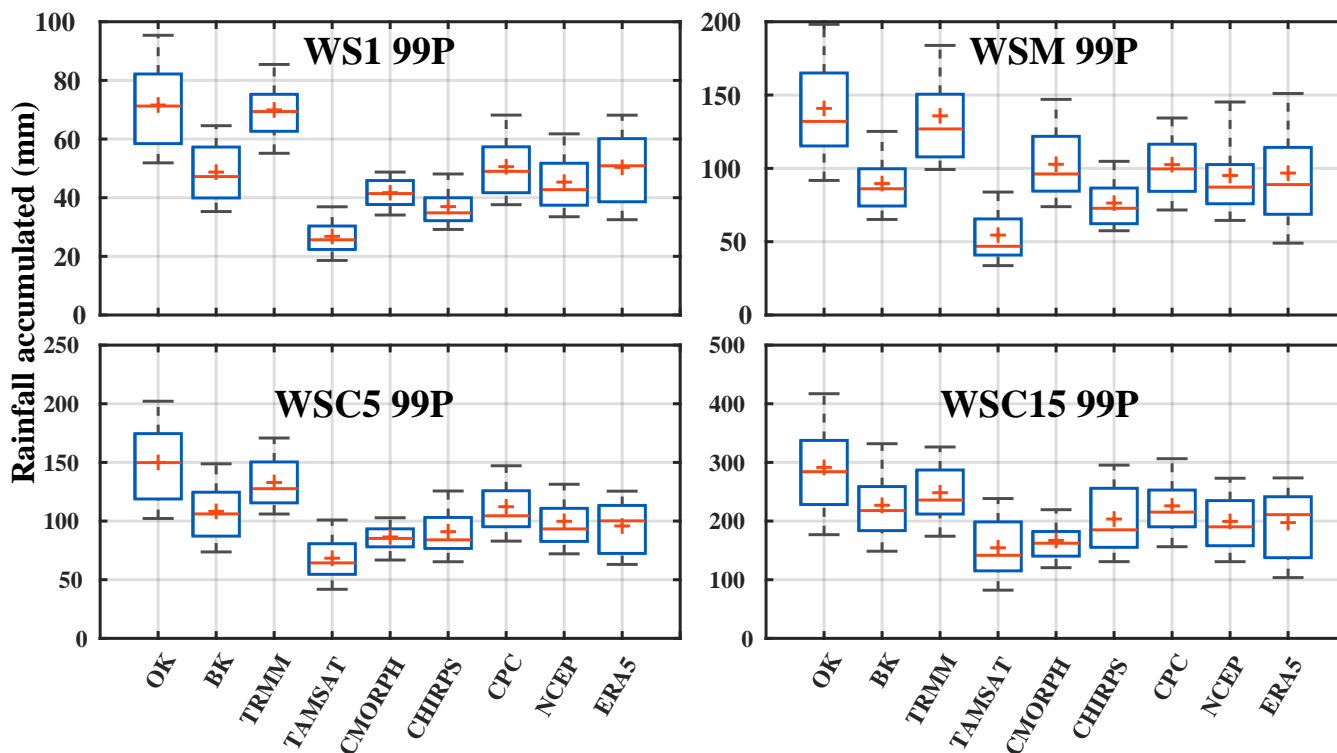
Figure 9. Yearly cumulated rainfall provided by WS1, WSM, WSC5 and WSC15 (99th) percentiles, averaged for the period 1998-2010, for : TRMM, TAMSAT, CMORPH, CHIRPS, CPC, NCEP, ERA5, BK, OK. The + represent the mean value, the − represent the median value, the box represents the 25th and 75th percentile values, and the "whiskers" represent the extreme values. Details on the datasets are provided in Table 1
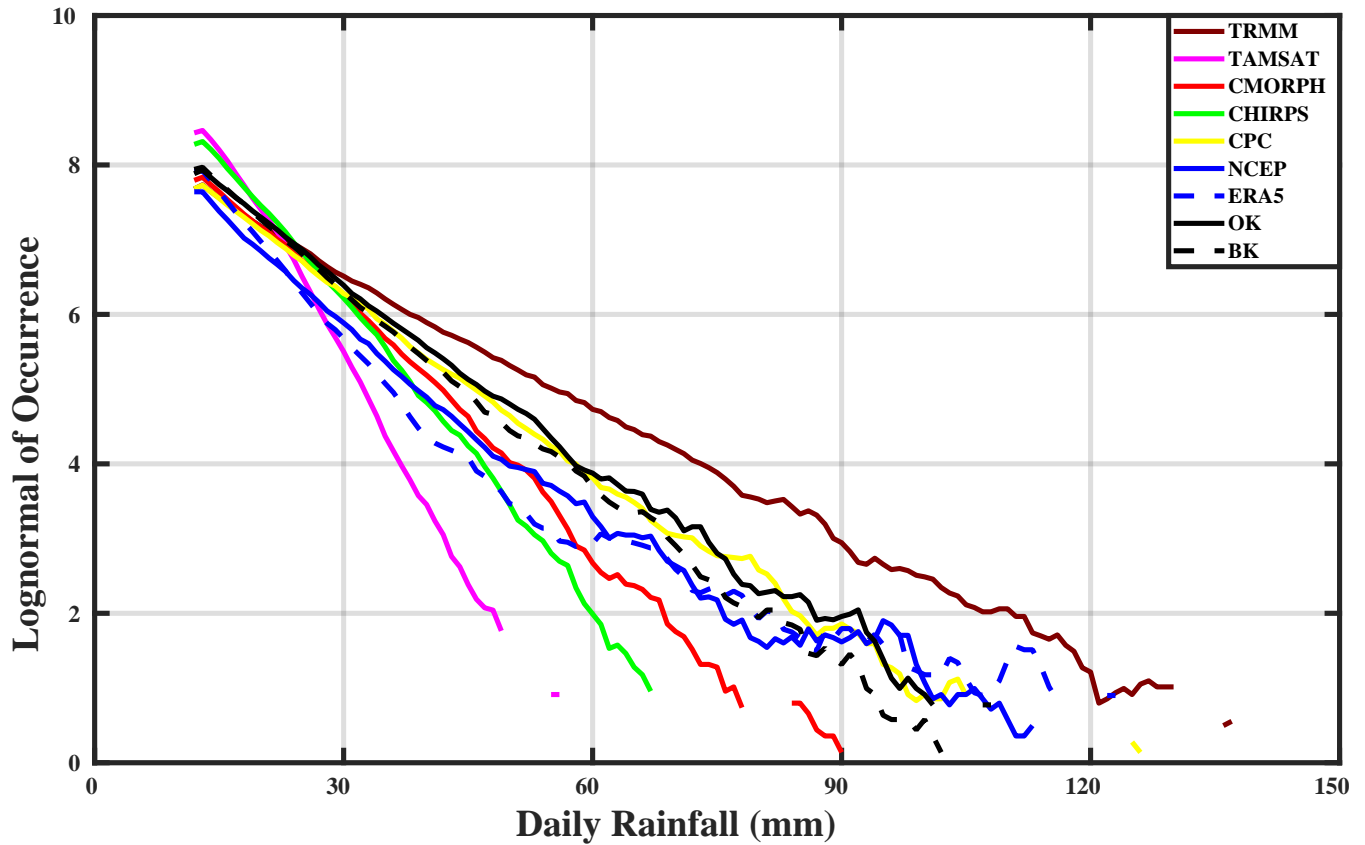
Figure 10. Comparison of the climatological distribution of intensities of daily rainfall (1998-2010) provided by TRMM, TAMSAT, CMORPH, CHIRPS, CPC, NCEP, ERA5, BK, OK over the Senegal. Details on the datasets are provided in Table 1

Figure 11. Taylor Diagram of the spatial distribution of the number of WSC5, WS1, WSM, WSC5 and WSC15 (99th) percentiles using TRMM, TAMSAT, CMORPH, CHIRPS, CPC, NCEP, ERA5, BK. OK product is considered as reference during the period 1998-2010. Details on the datasets are provided in Table 1
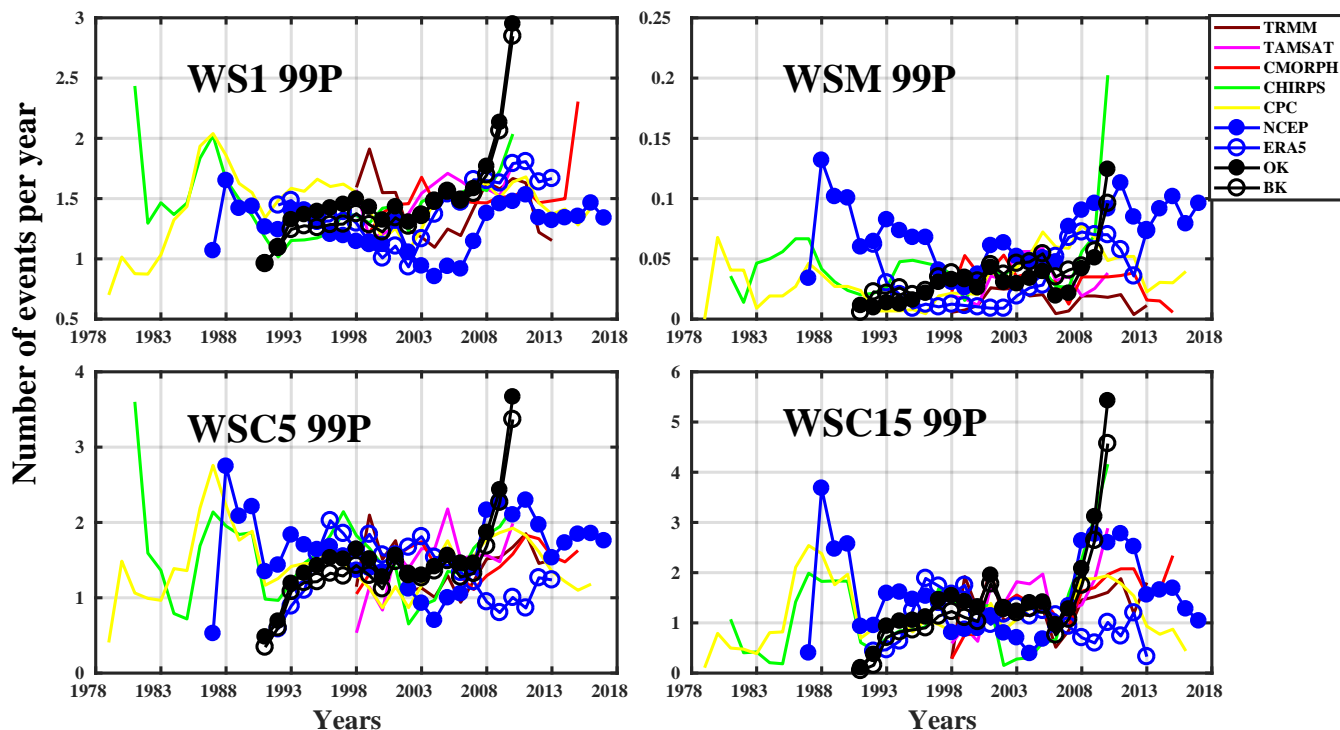
Figure 12. Interannual variability of the number of WS1, WSM, WSC5 and WSC15 (99th) percentiles derived from TRMM (1998-2013), TAMSAT(1998-2010), CMORPH (1998-2015), CHIRPS (1981-2010), CPC (1979-2016), NCEP (1992-2013), ERA5 (1987-2017), BK (1991-2010), OK (1991-2010). Details on the datasets are provided in Table 1

Table 1. Summary of the daily precipitation datasets used in this study

Name of datasets	Period of datasets	Spatial resolution	
TRMM 3B42 (V7)	1998 - 2013	*Daily*	$0.25^o \times 0.25^o$
CMORPH	1998 - 2015	*Daily*	$0.05^o \times 0.05^o$
CHIRPS	1981 - 2010	*Daily*	$0.05^o \times 0.05^o$
TAMSAT V3	1983 - 2016	*Daily*	$0.0375^o \times 0.0375^o$
CPC	1979 - 2017	*Daily*	$0.5^o \times 0.5^o$
NCEP	1992 - 2013	*Daily*	$0.1^o \times 0.1^o$
ERA5	1987 - 2017	*Daily*	$0.1^o \times 0.1^o$
OBS In Situ	1991 - 2010	*Daily*	65 Stations
Ordinary Kriging (OK)	1991 - 2010	*Daily*	$0.25^o \times 0.25^o$
Kriging (BK)	1991 - 2010	*Daily*	$0.25^o \times 0.25^o$

Table 2. Definition of indices to detect the Dry Spells

Dry Spells Indices	Definitions
DSC5	5 days with less than 5 mm of rainfall
DSC10	10 days with less than 10 mm of rainfall
DSC15	15 days with less than 15 mm of rainfall
DSC20	20 days with less than 20 mm of rainfall
DSs	1-3 consecutive dry days
DSm	4-7 consecutive dry days
DSl	8-14 consecutive dry days
DSxl	consecutive dry days exceding 15 days

Table 3. Definition of indices to detect the Wet Spells, XX for 90, 95, 99 and 99.5 percentiles

Wet Spells Indices	Definitions
WS1 *XX*P	1day with rainfall $> XX^{th}$p of daily rainfall
WSM *XX*P	2 day or more with rainfall $> XX^{th}$p of daily rainfall
WSC5 *XX*P	5-d precip. $> XX^{th}$p of 5-day cumulative rainfall
WSC10 *XX*P	10-d precip. $> XX^{th}$p of 10-day cumulative rainfall
WSC15 *XX*P	15-d precip. $> XX^{th}$p of 15-day cumulative rainfall
WSC20 *XX*P	20-d precip. $> XX^{th}$p of 20-day cumulative rainfall